NANO LETTERS

2007
Vol. 7, No. 9
2633−2637

Biomimetic Superhydrophobic Surfaces: Multiscale Approach

Michael Nosonovsky[†,‡] and Bharat Bhushan*[,‡]

National Institute of Standards and Technology, 100 Bureau Drive, Stop 8520, Gaithersburg, Maryland 20899-8520, and Nanotribology Laboratory for Information Storage and MEMS/NEMS(NLIM), The Ohio State University, 201 West 19th Avenue, Columbus, Ohio 43210-1142

Received May 1, 2007

ABSTRACT

Micro- and macrodroplet evaporation and condensation upon micropatterned superhydrophobic surfaces built of flattop pillars are investigated with the use of an environmental scanning electron microscope. It is shown that the contact angle hysteresis depends upon both kinetic effects at the triple line and adhesion hysteresis (inherently present even at a smooth surface) and that the magnitude of the two contributions is comparable. The transition between the composite (Cassie) and wetted (Wenzel) states is a linear effect with the microdroplet radius proportional to the pitch over pillar diameter. It is shown that wetting of a superhydrophobic surface is a multiscale phenomenon that involves three scale lengths. Although the contact angle is the macroscale parameter, the contact angle hysteresis and the Cassie–Wenzel transition cannot be determined from the macroscale equations and are governed by micro- and nanoscale effects.

Biological and artificial (biomimetic) micropatterned surfaces built of microscopic pillars are known to be extremely water repellent or superhydrophobic. A water droplet can roll on top of the pillars resulting in a high contact angle (CA) and low contact angle hysteresis (CAH), Figure 1a. Superhydrophobic micropatterned surfaces became a topic of active investigation in recent years due to their potential application for nanotechnology.[1,2] However, despite the apparent simplicity of these systems, there are still a number of effects related to superhydrophobicity that have no adequate explanation. One such effect is the transition between the Cassie state (composite interface with air pockets trapped under the droplet) and the Wenzel state (complete wetting of the surface). It is known from the experiments, that the transition from the Cassie to Wenzel state is an irreversible event.[2−4] Whereas such a transition can be induced, for example, by applying pressure or force to the droplet,[4] electric voltage,[5] or vibration,[6] the opposite transition has never been observed. Several approaches have been proposed to explain the Cassie−Wenzel transition, including net surface energy levels of the two states,[3] the balance between the droplet weight and surface tension force,[7] history of the system,[8] droplet curvature,[9] dynamic destabilizing effects and gradual stochastic transition,[10] and multiscale roughness.[11] Numerous experimental results support many of these approaches; however, there is still no convincing explanation of the mechanism of transition. We studied recently wetting of micropatterned Si surfaces and observed that wetting behavior depended upon a microscale nondimensional parameter, the spacing factor.[2] In the present work, we study experimentally and theoretically evaporation/condensation of microdroplets with an environmental scanning electron microscope (ESEM) and show that CAH and transition between wetting regimes are multiscale phenomena.

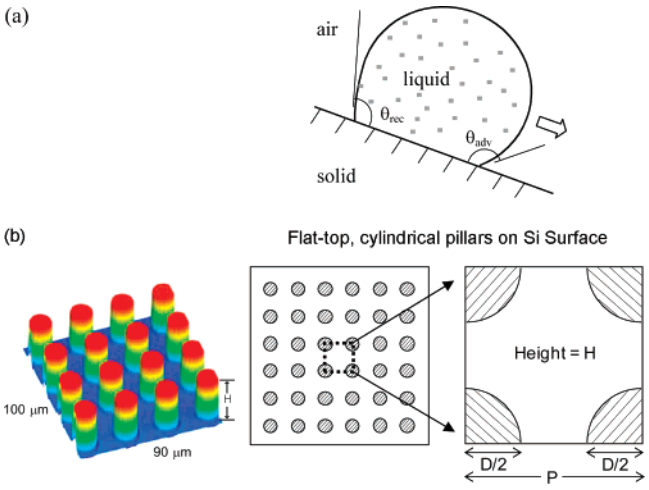

Figure 1. (a) Schematics of a droplet on a tilted substrate showing advancing (θ_{adv}) and receding (θ_{rec}) contact angles. The difference between these angles constitutes the contact angle hysteresis. (b) Optical profiler image of the patterned surface.

* Corresponding author: e-mail, bhushan.2@osu.edu; tel, 614 292 0651; fax, 614 292 0325.
† National Institute of Standards and Technology.
‡ The Ohio State University.

10.1021/nl071023f CCC: $37.00
Published on Web 08/17/2007

Table 1. Wetting of a Superhydrophobic Surface as a Multiscale Process

scale level	characteristic length	parameters	CAH mechanism	Cassie−Wenzel transition mechanisms
macroscale	droplet radius (mm)	contact angle, droplet radius	no CAH predicted	transition may occur at the intersection of the two regimes
microscale	micropattern detail (μm)	shape of the droplet, position of the liquid−vapor interface (h)	kinetic effects (pinning of the triple line)	kinetic effects, deposition of the droplet
nanoscale	molecular heterogeneity (nm)	molecular description	thermodynamic and dynamic effects, adhesion hysteresis	wetting−dewetting asymmetry, surface heterogeneity, dynamic effects

Unlike most classical systems studied by thermodynamics and statistical physics, a droplet upon a superhydrophobic surface is a multiscale system in a sense that its macroscale properties, such as the CA and CAH, cannot be determined only from macroscale equations, and thus it cannot be treated as a closed macroscale system (Table 1). While macroscale thermodynamic analysis allows predicting the CA for both Wenzel and Cassie states, the transitions between these two states and the CAH involve processes and instabilities at the micrometer scale (such as pinning of the triple line) and at the molecular scale (such as the inherent adhesion hysteresis).

We studied two series of patterned Si surfaces, covered with a monolayer of hydrophobic tetrahydroperfluorodecyltrichlorosilane (CA with a nominally flat surface, $\theta_0 = 109°$, advancing and receding CA are $\theta_{adv0} = 116°$ and $\theta_{rec0} = 82°$), formed by flat-top cylindrical pillars. Series 1 had pillars with the diameter $D = 5$ μm, height $H = 10$ μm, and

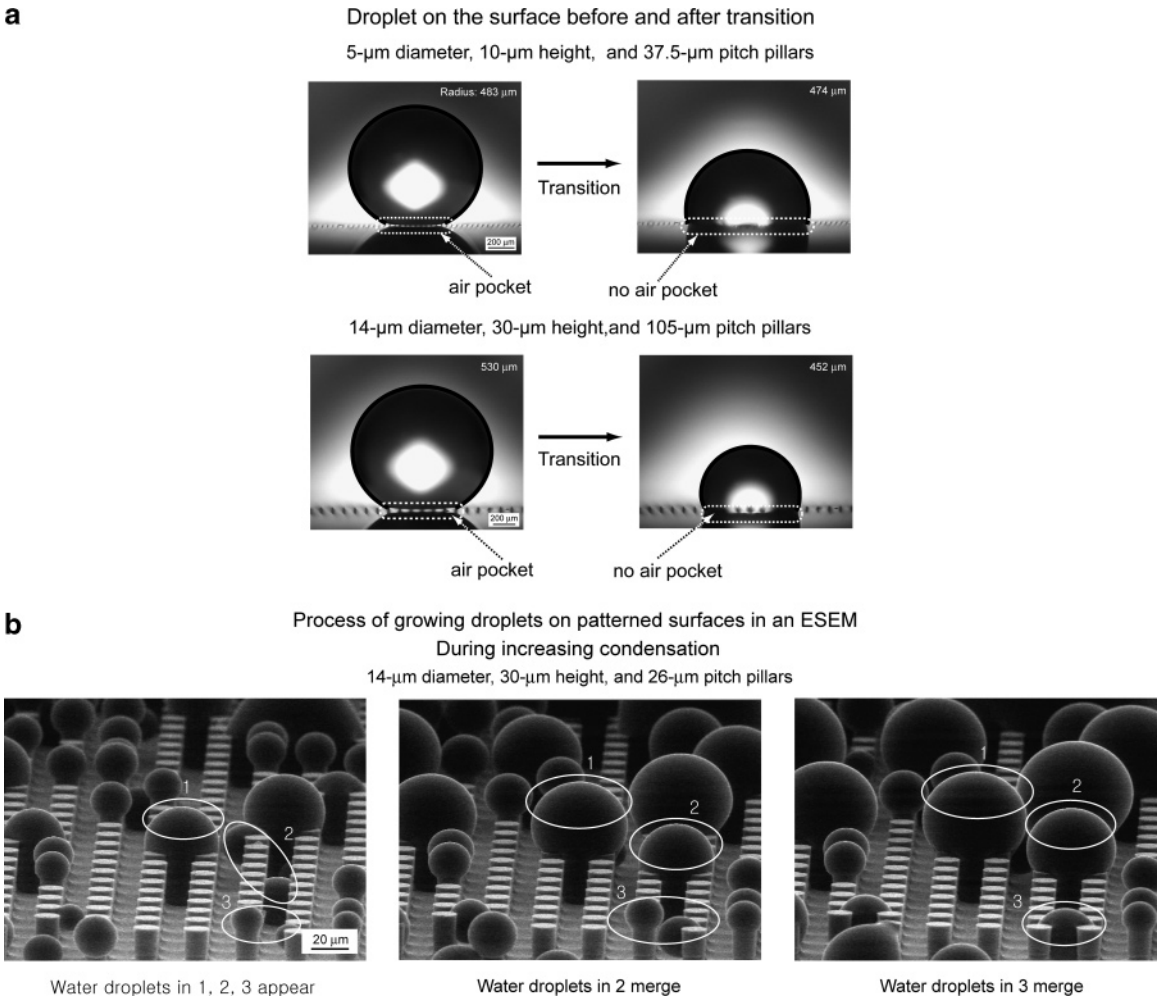

Figure 2. ESEM micrographs of microdroplets upon the patterned surface: (a) Cassie−Wenzel transition during evaporation. (b) Droplets grow and merge during condensation; however, no transition from Wenzel to Cassie regime takes place. The Cassie−Wenzel transition is irreversible due to the asymmetry of wetting and dewetting (Y. C. Jung and B. Bhushan, Ohio State University).

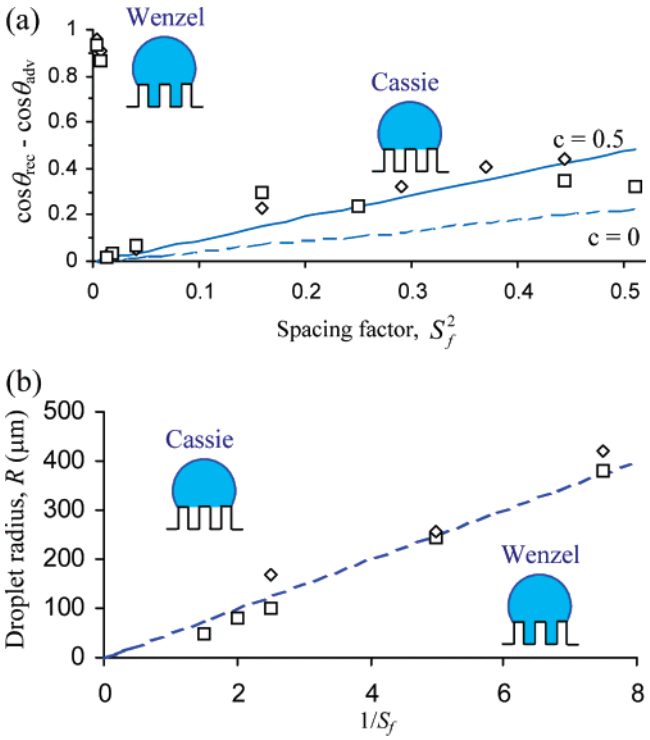

Figure 3. (a) CAH as a function of S_f for the first (squares) and second (diamonds) series of the experiments compared with the theoretically predicted values of $\cos\theta_{adv} - \cos\theta_{rec} = (D/P)^2(\pi/4)(\cos\theta_{adv0} - \cos\theta_{rec0}) + c(D/P)^2$, where c is a proportionality constant. It is observed that when only the adhesion hysteresis/interface energy term is considered ($c = 0$), the theoretical values are underestimated by about a half, whereas $c = 0.5$ provides a good fit. Therefore, the contribution of the adhesion hysteresis is of the same order of magnitude as the contribution kinetic effects. (b) Droplet radius, R, for the Cassie−Wenzel transition as a function of $P/D = 1/S_f$. It is observed that the transition takes place at a constant value of $RD/P \sim 50$ μm (dashed line). This shows that the transition is a linear phenomenon.

pitch values P = (7, 7.5, 10, 12.5, 25, 37.5, 45, 60, and 75) μm, while series 2 had $D = 14$ μm, $H = 30$ μm, P = (21, 23, 26, 35, 70, 105, 126, 168, and 210) μm (Figure 1b). It is convenient to introduce[2] the spacing factor $S_f = D/P$, and thus the fraction of the solid−liquid contact area is given by $f_{SL} = \pi S_f^2/4$ ($f_{SL} = 1$ for the Wenzel state and $0 < f_{SL} < 1$ for the Cassie state). The CA and CAH of millimeter-sized water droplets upon the samples were measured. In addition, CA and the Wenzel−Cassie transition during evaporation/condensation of microscale droplets were studied in the ESEM (Figure 2). We found that the CAH involves two terms (Figure 3a): the term $S_f^2(\pi/4)(\cos\theta_{adv0} - \cos\theta_{rec0})$, corresponding to the adhesion hysteresis (which is observed even at a nominally flat surface and is a result of molecular-scale imperfectness) and the term $H_r \propto D/P^2$ corresponding to microscale roughness and proportional to the edge line density. Thus the CAH is given by[2,12]

$$\cos\theta_{adv} - \cos\theta_{rec} = \frac{\pi}{4}S_f^2(\cos\theta_{adv0} - \cos\theta_{rec0}) + H_r \quad (1)$$

where θ_{adv0}, θ_{rec0}, θ_{adv}, and θ_{rec} are advancing and receding contact angles for the corresponding smooth and rough surfaces. The droplet radius, R, at the Cassie−Wenzel transition was observed to be proportional to P/D (or P/H) (Figure 3b), which suggests that the transition is a linear phenomenon and that neither droplet droop (that would involve P^2/H) nor droplet weight (that would involve R^3) are responsible for the transition, but rather linear geometric relations are involved.

The CAH is a result of the wetting/dewetting asymmetry that leads also to the asymmetry of the Wenzel and Cassie states. While the fragile metastable Cassie state is often observed, as well as its transition to the Wenzel state, the opposite transition never happens. The CA with our patterned surfaces, θ, is related to that with a nominally flat surface, θ_0, by

$$\cos\theta = (1 + 2\pi S_f^2)\cos\theta_0 \quad \text{(Wenzel state)} \quad (2)$$

$$\cos\theta = \frac{\pi}{4}S_f^2(\cos\theta_0 + 1) - 1 \quad \text{(Cassie state)} \quad (3)$$

For a perfect macroscale system, the transition between the Wenzel and Cassie states should occur only at the intersection of the two regimes (the point, at which the CA and net energies of the two regimes are equal, corresponding to $S_f = 0.51$). It is observed, however, that the transition from the metastable Cassie to stable Wenzel occurs at much lower values of the spacing factor $0.083 < S_f < 0.111$. As shown in Figure 4a, the stable Wenzel state (i) can transform into the stable Cassie state with increasing S_f (ii). The metastable Cassie state (iii) can abruptly transform (iv) into the stable Wenzel state. The transition (i−ii) corresponds to equal Wenzel and Cassie states free energies, whereas the transition (iv) corresponds to the Wenzel energy much lower than the Cassie energy and thus involves significant energy dissipation and is irreversible. The solid and dashed straight lines correspond to the values of the CA, calculated from eqs 2 and 3 using the CA for a nominally flat surface, $\theta_0 = 109°$. The two series of the experimental data are shown with squares and diamonds.

Figure 4b shows the values of the CA after the transition took place (dimmed blue squares and diamonds), as it was observed during evaporation in the ESEM. For both series, the values almost coincided. For comparison, the values of the receding CA measured for millimeter-sized water droplets are also shown (squares and diamonds), since evaporation constitutes removing liquid and thus the CA during evaporation should be compared with the receding CA. The solid and dashed straight lines correspond to the values of the CA, calculated from eqs 2 and 3 using the receding CA for a nominally flat surface, $\theta_{rec0} = 82°$. Both parts a and b of Figure 4 demonstrate a good agreement between the experimental data and eqs 2 and 3.

In order to understand the CAH and transition between the Cassie and Wenzel states, the shape of the free surface energy profile can be analyzed. The free surface energy of a droplet upon a smooth surface as a function of the CA has a distinct minimum, which corresponds to the most stable CA.[13] As shown in Figure 4c, the macroscale profile (smooth

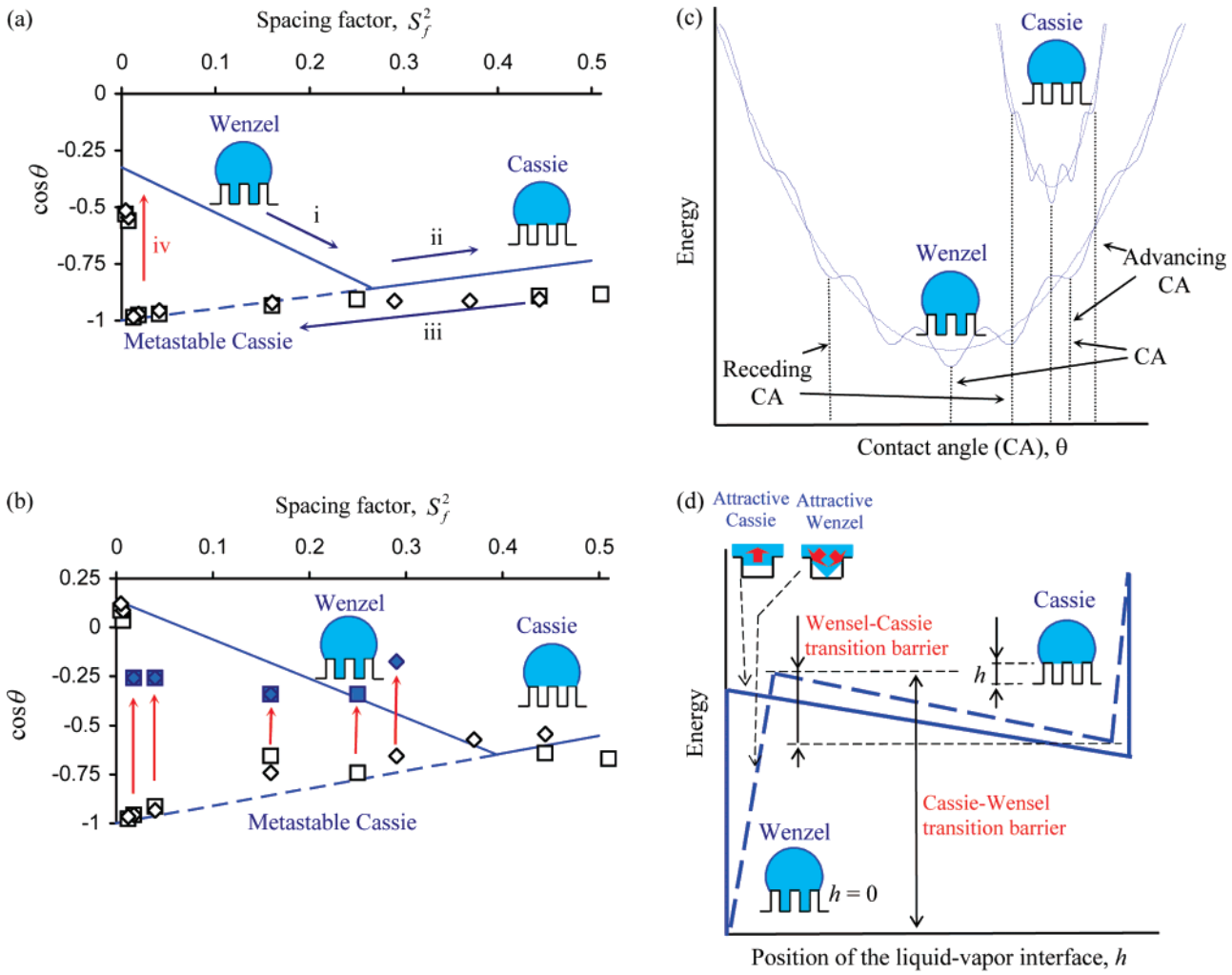

Figure 4. (a) Wetting-dewetting hysteresis for a superhydrophobic surface. Theoretical (solid and dashed) and experimental (squares for the first series, diamonds for the second series) CA as a function of the spacing factor. (b) Receding CA and values of the CA observed after the transition during evaporation (blue). (c) Schematics of net free energy profiles as a function of the CA for macroscale (smooth line) and microscale (wavy line) profiles. (d) The two branches (Wenzel and Cassie) are found when a dependence of energy upon h is introduced,[10−11] for the microscale description of the liquid−vapor interface as a horizontal plane (solid line) and interface with nanoscale imperfectness (dashed line).

line) of the net surface energy allows us to find the CA (corresponding to energy minimums); however it fails to predict the CAH and Cassie−Wenzel transition, which are governed by micro- and nanoscale effects. The microscale energy profile (wavy line) has numerous energy maxima and minima due to the surface micropattern. While exact calculation of the energy profile for a three-dimensional droplet is complicated, a qualitative shape may be obtained by assuming a periodic sinusoidal dependence,[13] superimposed upon the macroscale profile, as shown in Figure 4c by the wavy line. The largest and smallest values of the energy minimums correspond to the advancing and receding contact angles.

The energy profile as a function of the CA does not provide any information on how the transition between the Cassie and Wenzel states occurs, because there two states correspond to completely isolated branches of the energy profile in Figure 4c. However, the energy may depend not only upon the CA but also upon micro/nanoscale parameters, such as, for example, the vertical position of the liquid−vapor interface under the droplet, h (assuming that the interface is a horizontal plane), or similar geometrical parameters (assuming a more complicated shape of the interface). As observed from Figure 4d, for the horizontal interface, only the Cassie state serves as an attractor for the system, whereas as soon as a more complicated shape is introduced (due to nanoscale imperfectness or dynamic effects such as the capillary waves[10]), for example, the "triangular" shape as shown in Figure 4d, the Wenzel state may become the second attractor for the system. The energy barrier for the Wenzel−Cassie transition is much smaller than that for the opposite transition, which explains the irreversibility of the transition.

To summarize, we showed that CAH and the Cassie−Wenzel transition cannot be determined from the macroscale equations and are governed by micro- and nanoscale phenomena. Our theoretical arguments are supported by our experimental data on micropatterned surfaces.

Acknowledgment. The authors thank Mr. Yong-Chae Jung from The Ohio State University, who conducted most of the experimental measurements used in this Letter.

References

(1) Burton, Z.; Bhushan, B. Hydrophobicity, Adhesion, and Friction Properties of Nanopatterned Polymers and Scale Dependence for Micro- and Nanoelectromechanical Systems. *Nano Lett.* **2005**, *5*, 1607−1613.
(2) Bhushan, B.; Nosonovsky, M.; Jung Y.-C. Towards Optimization of Patterned Superhydrophobic Surfaces. *J. R. Soc. Interface* **2007**, *4*, 643−648.
(3) Lafuma, A.; Quèrè, D. Superhydrophobic States. *Nat. Mater.* **2003**, *2*, 457−460.
(4) Barbieri, L.; Wagner, E.; Hoffmann, P. Water Wetting Transition Parameters of Perfluorinated Substrates with Periodically Distributed Flat-Top Microscale Obstavles. *Langmuir* **2007**, *23*, 1723−1734.
(5) Bahadur, V.; Garimella, S. V. Electrowetting-Based Control of Static Droplet States on Rough Surfaces. *Langmuir* **2007**, *23*, 4918−4924.
(6) Bormashenko, E.; Pogreb, R.; Whyman, G.; Erlich, M. Cassie-Wenzel Wetting Transition in Vibrated Drops Deposited on the Rough Surfaces: Is Dynamic Cassie-Wenzel Transition 2D or 1D Affair? *Langmuir* **2007**, *23*, 6501−6503.
(7) Extrand, C. W. Model for Contact Angles and Hysteresis on Rough and Ultraphobic Surfaces. *Langmuir* **2002**, *18*, 7991−7999.
(8) Patankar, N. A. Transition Between Superhydrophobic States on Rough Surfaces. *Langmuir* **2004**, *20*, 7097−7102.
(9) Quéré, D. Non-Sticking Drops. *Rep. Prog. Phys.* **2005**, *68*, 2495−2535.
(10) Nosonovsky, M.; Bhushan, B. Stochastic model for metastable wetting of roughness-induced superhydrophobic surfaces. *Microsyst. Technol.* **2006**, *12*, 231−237.
(11) Nosonovsky, M Multiscale roughness and stability of superhydrophobic biomimetic interfaces. *Langmuir* **2007**, *23*, 3157−3161.
(12) Nosonovsky, M. Model for Solid-Liquid and Solid-Solid Friction for Rough Surfaces with Adhesion Hysteresis. *J. Chem. Phys.* **2007**, *126*, 224701.
(13) Johnson, R. E.; Dettre, R. H. Contact Angle Hysteresis. *Contact Angle, Wettability, and Adhesion*; Fowkes, F. M., Ed.; Advances in Chemistry Series 43; American Chemical Society: Washington, DC, 1964; pp 112−135.

NL071023F